Interacting Multiple Model Seeker Filter For Homing Guidance

S.K. Kashyap[a,1], N. Shanthakumar[b], VPS Naidu[c], Girija G[d].

[a ,b,c,d] Multi Sensor Data Fusion Group, Flight Mechanics and Control Division, National Aerospace Laboratories, Bangalore

Abstract: In this paper, IMM based Augmented Extended Kalman Filter (IMM-AEKF) RF seeker filter is designed to operate in close loop homing guidance to track highly maneuvering Air Breathing Targets (ABT). The performance of the seeker filter is evaluated with six degree of freedom interceptor-target engagement simulation with seeker filter in closed guidance loop of the interceptor. Different filter performance criteria have been used to verify the performance of the seeker filter. Sensitivity/robustness of the seeker filter to various design parameters has been evaluated. IMM-AEKF was found to efficiently handle the various seeker noise and achieve miss distances that are acceptable for several realistic engagement scenario.

Key words: Seeker Filter, Homing Guidance, Turn Rate, Attenuation Factor

1 INTRODUCTION

RF (radio frequency) seeker filter design for homing guidance requirements are highly demanding and challenging [1-2,12]. Very low filter lag and high attenuation of seeker noise are some of the challenges that need to be addressed. Over and above, there will be periodic data loss due to eclipsing in RF seeker. Air breathing targets against which homing guidance with seeker filter is required are capable of performing evasive maneuver. This leads to purely reactive target state estimation, often producing sluggish state estimator response in the presence of agile targets. An ideal approach to preserving the agility of the target state estimator without sacrificing its accuracy is to model the target motion with multiple target motion models that characterize the target motion all the time and a switching logic. The switching logic is then allowed to select any one of these models at any instant of time. Thus, to an estimator, at each time instant, the target motion model appears to follow one of these models. The resulting target state estimator in this case consists of a bank of Kalman filters whose outputs are blended using a hypothesis-testing algorithm. This approach is called Interacting Multiple Model (IMM) estimation technique [3].

The physical model of the target motion is assumed to be known, but the exact maneuver strategy is parameterized and then determined online together with the target states. Since the target maneuvering logic is adaptively determined, the resulting estimation scheme can be expected to have agile response to any changes in the target behavior and there by filter time lag is expected to be well under control.

This paper presents a two model based interacting multiple model seeker filter with extended Kalman filter as mode-matched filter which operates in closed homing guidance loop to generate required guidance commands to intercept maneuvering air-breathing target. The major challenge in processing the RF seeker data, especially in end game, is glint noise [4] which is a non-Gaussian noise with heavy tail distribution. The glint noise is a function of target aspect, RCS fluctuation and range to go. Obviously, when the range to go is less, the effect of glint noise (if not accounted properly) on guidance will be more and this would in turn result in large miss distances. To overcome this problem, the glint noise and radar cross section (RCS) fluctuations present in seeker data are handled as augmented states and estimated in the filter algorithm and hence the filter algorithm is named as IMM-AEKF. The two models in IMM-AEKF consists constant acceleration (CA) and constant jerk (CJ) models as target motion models [4]. The performance of the seeker filter is verified with six degree of freedom interceptor-target engagement simulation with seeker filter in guidance loop of the interceptor. Different sensitivity study and filter performance criteria have been used to verify the performance of the seeker filter.

2 IMM BASED SEEKER FILTER DESIGN

In target tracking applications, Kalman filters are extensively used. In general target tracking applications, the

Email addresses: sudesh@nal.res.in (First Author),
nskumar@nal.res.in (Second Author),
vpsnaidu@nal.res.in (Third Author)
ggirija@nal.res.in (Forth Author)
URL: http://www.nal.res.in
[1]Corresponding author

state of the target includes its position and the time-derivatives of position. For targets moving with constant velocity (CV), the state model includes the first derivative of position and for targets moving with constant acceleration (CA) it includes second derivative of position. Models with second order derivatives are preferred for tracking maneuvering targets and referred to as acceleration models. However, for rapidly maneuvering targets, higher order derivatives of position become significant. Hence models which include third order derivative of the target position, termed constant jerk (CJ) models are preferred for tracking targets executing rapid/evasive maneuvers [5].

When the target is maneuvering randomly, adaptive state estimation is required to track a target whose behavior pattern keeps changing with time. The Interacting Multiple Model (IMM) [6] is one such adaptive estimator which is based on the assumption that a finite number of models are required to characterize the target motion at all times. IMM approach is a sub-optimal hybrid estimator since it is characterized by both continuous valued parameters like target position, velocity and accelerations defined by the difference or differential form of state equations, as well as by the discrete stochastic process that controls the selection of a model corresponding to each behavior mode. The IMM approach, thus, performs both target state estimation as well as model selection from a given set of models. The "model set" may consist of several models, such as a CV model, CA model, CJ model and a coordinated turn (CT) model. A finite state Markov chain with known transition probabilities is used to switch from one model to another. The mode transition probabilities, which constitute the transition matrix, are the design parameters for the algorithm. Thus, the IMM algorithm, in general, consists of a set of mode matched filter modules that interact in a certain way to yield the mode-conditioned state estimates. The individual mode matched filters can either be Kalman Filters (KF) or Extended Kalman Filters (EKF) or Augmented Kalman filter (AEKF) as in the present case. The two model based IMM algorithm structure and flow chart is shown in Fig. 1. The description of IMM filter algorithm is given in [7].

2.1 Target Motion Model

The base state model for a fixed-structure hybrid system can be described as follows

$$\begin{aligned} X(k+1) &= F_j(k)X(k) + G_j(k)w_j(k) \quad \forall\ j \in M \\ Z(k) &= h(X(k)) + v_j(k) \qquad\quad \forall\ j \in M;\quad j = 1,\ldots r \end{aligned} \tag{1}$$

where, M is a set of possible r modes and G_j denotes the process noise gain matrix. The process and measurement noises are Gaussian, mutually uncorrelated with zero mean and known covariances. The function h represents the nonlinear relation between the states X and the measurements Z. It is clear from (1) that the system

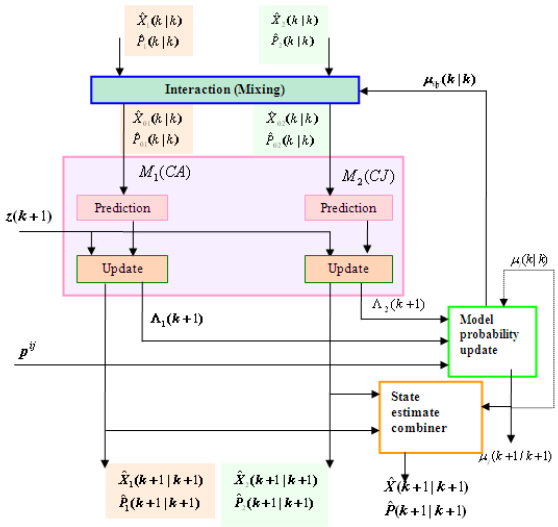

Figure 1 IMM Block Diagram

transition matrix F and the noise statistics can differ from mode to mode.

State Model: State vector for CA model is

$$X_1 = \begin{bmatrix} \Delta x,\ \Delta\dot{x},\ a_{tx},\ \Delta y,\ \Delta\dot{y},\ a_{ty},\ \Delta z,\ \Delta\dot{z},\ a_{tz}, \\ 6 \text{ additional (augmented) states to account glint \& RCS noise} \end{bmatrix}$$

State vector for CJ model is

$$X_2 = \begin{bmatrix} \Delta x,\ \Delta\dot{x},\ a_{tx},\ j_{tx},\Delta y,\ \Delta\dot{y},\ a_{ty},\ j_{ty},\Delta z,\ \Delta\dot{z},\ a_{tz},\ j_{tz}, \\ 6 \text{ augmented states to account glint \& RCS noise} \end{bmatrix}$$

Model 1: Constant Acceleration (CA) Model

$$\begin{aligned} \Delta\dot{x} = \Delta V_x;\ \Delta\dot{V}_x = a_{tx} - a_{mx};\ \dot{a}_{tx} = -\left(\frac{a_{tx}}{\tau_x}\right);\ \dot{j}_{tx} = 0 \\ \Delta\dot{y} = \Delta V_y;\ \Delta\dot{V}_y = a_{ty} - a_{my};\ \dot{a}_{ty} = -\left(\frac{a_{ty}}{\tau_y}\right);\ \dot{j}_{ty} = 0 \\ \Delta\dot{z} = \Delta V_z;\ \Delta\dot{V}_z = a_{tz} - a_{mz};\ \dot{a}_{tz} = -\left(\frac{a_{tz}}{\tau_z}\right);\ \dot{j}_{jz} = 0 \end{aligned} \tag{2}$$

Model 2: Constant Jerk (CJ) Model

$$\begin{aligned} \Delta\dot{x} = \Delta V_x;\ \Delta\dot{V}_x = a_{tx} - a_{mx};\ \dot{a}_{tx} = j_{tx};\ \dot{j}_{tx} = -\left(\frac{j_{tx}}{\tau_x}\right) \\ \Delta\dot{y} = \Delta V_y;\ \Delta\dot{V}_y = a_{ty} - a_{my};\ \dot{a}_{ty} = j_{ty};\ \dot{j}_{ty} = -\left(\frac{j_{ty}}{\tau_y}\right) \\ \Delta\dot{z} = \Delta V_z;\ \Delta\dot{V}_z = a_{tz} - a_{mz};\ \dot{a}_{tz} = j_{tz};\ \dot{j}_{jz} = -\left(\frac{j_{tz}}{\tau_z}\right) \end{aligned} \tag{3}$$

where, $\Delta x, \Delta y, \Delta z$ are the relative positions of the target w.r.t interceptor along three Cartesian coordinates and

$\Delta V_x, \Delta V_y, \Delta V_z$ are the relative velocities of target w.r.t. interceptor, a_{tx}, a_{ty}, a_{tz} are the target accelerations, j_{tx}, j_{ty}, j_{tz} are the target jerks, a_{mx}, a_{my}, a_{mz} are the missile (interceptor) accelerations, and τ_x, τ_y, τ_z are the correlation time constants.

Augmented Model: State model for target motion is extended with 6 augmented states to account for coloured process noise with RCS fluctuation and glint effect present in the seeker data. The first two states corresponding to RCS fluctuation can be represented as the sum of squares of two identical independent normal stochastic 1st order Markov processes with zero mean and standard deviation of $2\sigma_{av}$ (σ_{av} is the mean RCS value of target), i.e.

$$\begin{aligned}\sigma(k) &= \xi_1^2(k) + \xi_2^2(k)\\ \xi_1(k) &= \rho\xi_1(k-1) + N_1(0,1)\sqrt{(1-\rho^2)2\sigma_{av}}\\ \xi_2(k) &= \rho\xi_2(k-1) + N_2(0,1)\sqrt{(1-\rho^2)2\sigma_{av}}\end{aligned} \quad (4)$$

where, k is the scan number, $N_1(0,1)$ and $N_2(0,1)$ are white Gaussian noises (zero mean and unit standard deviation) with different seed numbers and $\xi_1(0) = \xi_2(0) = \sqrt{\sigma_{av}}/2$. Similarly glint noise model (for remaining 4 states of an augmented model) is conceptualised using 2nd order Markov process, RCS fluctuation, target aspect, length of target and range-to-go. The auto-correlation function of glint noise is given by:

$$\rho = e^{-2\pi B_T \tau} \quad (5)$$

where, B_T is one sided band on a half power level = 1 to 1.2 times B_C. The standard deviation of glint noise in linear units is given as:

$$\sigma_{gl\,\text{int}} = \sqrt{\frac{LengthT\arg et}{2\lambda\sqrt{2\pi}}} \quad (6)$$

where, $LengthT\arg et$ is the length of target chosen as = 10m and λ (λ=0.01742 m) is the wave length of received signal. Following equations are used for generation of glint noise

$$Gl\,int = \frac{\alpha_{t\arg et} LengthT\arg et}{10R_{TM}}\left(\frac{\xi_1(k)\xi_3(k)+\xi_2(k)\xi_4(k)}{\xi_1^2(k)+\xi_2^2(k)+0.05}\right) \quad (7)$$

$$\begin{aligned}\xi_3(k) &= b_{1g}\xi_3(k-1) + b_{2g}\xi_3(k-2) + a_{0g}N_3(0,1)(k) + a_{1g}N_3(0,1)(k-1)\\ \xi_4(k) &= b_{1g}\xi_3(k-1) + b_{2g}\xi_3(k-2) + a_{0g}N_4(0,1)(k) + a_{1g}N_4(0,1)(k-1)\end{aligned} \quad (8)$$

$$a_{0g} = \sigma_{gl\,\text{int}}\, alf \quad ; \quad a_{1g} = \sigma_{gl\,\text{int}}\,\frac{alf_0}{alf} \quad (9)$$

$$b_{1g} = 2\rho \quad ; \quad b_{21g} = -\rho^2 \quad (10)$$

$$\begin{aligned}alf &= \sqrt{\frac{alf_1+\sqrt{alf_1^2-4alf_0^2}}{2}} \quad ;\\ alf_0 &= \rho(\rho^2-1) - 2\pi B_T(1+\rho^2)\rho\tau \;;\; alf_1 = 1-\rho^4 + 4\rho^2(2\pi B_T\tau)\end{aligned} \quad (11)$$

where, ρ is the auto-correlation function of glint noise, $N_3(0,1)$ and $N_4(0,1)$ are the white Gaussian noises (zero mean and unit standard deviation) with different seed numbers, R_{TM} is the true relative missile range w.r.t. target in LOS frame at k th scan number and α_{target} = 0.2 is the target aspect with respect to the seeker and $\xi_3(0) = \xi_4(0) = 0$. The process noise covariance matrix 'Q' for CA model is 100*diag[0.0, 5.5555e-3, 0.05, 5.5555e-3, 0.0, 5.5555e-3, 0.05, 5.5555e-3, 0.0, 5.5555e-3, 0.05, 5.5555e-3, 1e-3, 1e-3, 1e-3, 1e-3, 1e-3, 1e-3] and 10 times 'Q' of CA for CJ model. Initial value of all the diagonal elements of a state error covariance matrix 'P' is kept at 1000.

Measurement model: Measurement vector consists of $\begin{bmatrix}\rho & \dot{\rho} & \phi_y & \phi_z & \dot{\phi}_{y_{ig}} & \dot{\phi}_{z_{ig}}\end{bmatrix}$ during non-eclipsing period and $\begin{bmatrix}\rho & \dot{\rho} & \phi_y & \phi_z\end{bmatrix}$ during eclipsing period. Where, ρ is range-to-go - distance between interceptor and target $\dot{\rho}$ is range rate, ϕ_y and ϕ_z are gimbal angles in yaw and pitch planes respectively, $\dot{\phi}_{y_{ig}}$ and $\dot{\phi}_{z_{ig}}$ are the respective line of sight (LOS) rates in inner gimbal frame. The relative position and velocity states of the target w.r.t interceptor in inertial frame is transformed to LOS frame using:

$$\begin{aligned}\rho &= \sqrt{\Delta x^2+\Delta y^2+\Delta z^2} \;;\; \dot{\rho} = \frac{\Delta x\Delta\dot{x}+\Delta y\Delta\dot{y}+\Delta z\Delta\dot{z}}{\rho}\\ \lambda_e &= \tan^{-1}\left(\frac{\Delta z}{\sqrt{\Delta x^2+\Delta y^2}}\right) \;;\; \lambda_a = \tan^{-1}\left(\frac{\Delta y}{\Delta x}\right)\\ \dot{\lambda}_e &= \frac{\Delta\dot{z}\left(\Delta x^2+\Delta y^2\right)-\Delta z\left(\Delta x\Delta\dot{x}+\Delta y\Delta\dot{y}\right)}{\rho^2\sqrt{\Delta x^2+\Delta y^2}} \;;\; \dot{\lambda}_a = \frac{\left(\Delta x\Delta\dot{y}-\Delta y\Delta\dot{x}\right)}{\sqrt{\Delta x^2+\Delta y^2}}\end{aligned} \quad (12)$$

The measurement model during non-eclipsing period is:

$$\begin{bmatrix}\rho\\ \dot{\rho}\end{bmatrix}_m = \begin{bmatrix}\rho\\ \dot{\rho}\end{bmatrix}; \begin{bmatrix}\phi_y\\ \phi_z\end{bmatrix}_m = \begin{bmatrix}\phi_y\\ \phi_z\end{bmatrix};$$

$$\begin{bmatrix}0\\ \dot{\phi}_{y_{ig}}\\ \dot{\phi}_{z_{ig}}\end{bmatrix}_m = C_f^g\, C_b^f\, C_i^b\, C_l^i \begin{bmatrix}-\dot{\lambda}_a \sin\lambda_e\\ \dot{\lambda}_e\\ \dot{\lambda}_a \cos\lambda_e\end{bmatrix} \quad (13)$$

The measurement model during eclipsing period is:

$$\begin{bmatrix}\rho\\ \dot{\rho}\end{bmatrix}_m = \begin{bmatrix}\rho\\ \dot{\rho}\end{bmatrix}; \qquad \begin{bmatrix}\phi_y\\ \phi_z\end{bmatrix}_m = \begin{bmatrix}\phi_y\\ \phi_z\end{bmatrix} \tag{14}$$

where, $\phi_y = tan^{-1}\left(\frac{m}{l}\right)$; $\phi_z = tan^{-1}\left(\frac{n}{\sqrt{l^2+m^2}}\right)$

and $\begin{bmatrix}l\\ m\\ n\end{bmatrix} = C_b^f C_i^b C_l^i \begin{bmatrix}1\\ 0\\ 0\end{bmatrix}$ (15)

where DCMs $C_f^g, C_b^f, C_i^b, C_l^i$ are defined in [8]. The RF Using above model, seeker measurements are generated with a help of 6dof missile simulator platform. It is observed that the measurement noise for range and range rate are white and Gaussian in nature, whereas noise for gimbal angles and LOS rates are coloured and with non-Gaussian distribution. In present case, the measurement noise covariance matrix $R = diag[5.2e3 \quad 2.06e2 \quad 5.0e-4 \quad 4.2e-4 \quad 0.0142 \quad 0.0166]$ is selected as a tuning parameter of IMM-AEKF. The desired value of 'R' is obtained by trial and error method while satisfying the stringent requirements such as maximum noise attenuation and minimum miss distance.

3 RF SEEKER DATA SIMULATION

Six Degree of Freedom (DoF) simulation code of air-to-air intercepting missile in FORTRAN and IMM-AEKF seeker filter in MATLAB® are integrated to simulate close loop interceptor-target engagement and the seeker filter performance is validated using several realistic interceptor-target engagement scenarios. Fig. 2 shows the block diagram of interceptor-target engagement simulation setup with seeker filter in the closed loop. Table 1 gives the different interceptor-target engagement scenarios considered for the present study. In order to simulate realistic target-interceptor engagement, the points need to be considered are: i) In the presence of adversary (intercepting missile), the target generally executes a turn and accelerates at short range to go ($R_{to\text{-}go} \approx 2$ km), ii) Target turns (velocity vector) at the rate of 20 to 25 deg/sec at a speed of 300 to 400 kmph and iii) Target under goes maximum roll rate to generate glint effect.

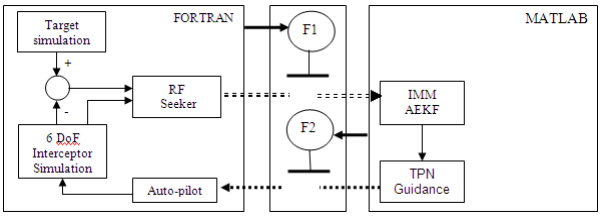

Figure 2 Simulation diagram

The target performing evasive maneuver is simulated within the permissible 'g' limit of a typical fighter aircraft at different altitudes as shown in Table 1. The target starts maneuver continuously with the 'g' profile given in Table 1 once the specified $R_{to\text{-}go}$ is reached. Proportional Navigation (PN) Guidance law is used to navigate the missile.

Case No.	Altitude (km)	Target Speed (kmph)	Maneuver (g's) pitch	yaw	Turn Rate (d/s)	Maneuver starts at $R_{to\text{-}go}$ (km)
1	0.5	485	6	-6	24.6	10
2	0.5	485	6	-6	24.6	5
3	0.5	485	6	-6	24.6	2.5
4	5.0	500	6	-6	23.7	10
5	5.0	500	6	-6	23.7	5
6	5.0	500	6	-6	23.7	2.5
7	10.0	540	6	-6	22.1	10
8	10.0	540	6	-6	22.1	5
9	10.0	540	6	-6	22.1	2.5
10	15.0	540	6	-6	22.1	10
11	15.0	540	6	-6	22.1	5
12	15.0	540	6	-6	22.1	2.5

Table 1 Engagement Simulation Parameters

4 PERFORMANCE OF IMM-AEKF SEEKER FILTER

The performance of the IMM-AEKF seeker filter is evaluated with 50 Monte-Carlo simulations in each case of interceptor-target engagement. Filter performance criteria [9-10] like percentage fit error (PFE), state error with bounds, innovation sequence with bounds, auto correlation of innovation sequence with bounds, root sum of squares position error (RSSPE), and miss distance and noise attenuation achieved are considered to verify the performance of the seeker filter. Fig. 3 shows the interceptor-target engagement in 3D (for case no. 1 from Table 1). Table 2 gives the percentage fit error obtained with IMM-AEKF seeker filter (for simulation cases 1 and 4 from Table 1). Seeker measurements are highly noisy characterized by correlated thermal noise and RCS fluctuations and one of the important demand from seeker filter is to achieve very high noise attenuation.

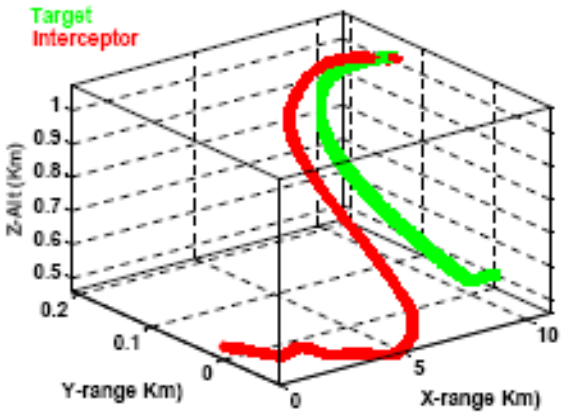

Figure 3 Interceptor-target engagement trajectory in 3D -case 1 (Table 1)

The noise attenuation factor (AF) defined below is less than 0.1 most of the time which indicates that 90% of noise has been attenuated.

$AF = \left(\frac{Y_t - \hat{Y}}{Y_t - Z} \right)$. where, Y_t, $\hat{Y}$ and Z are the true, estimated and measured value of the seeker output. Fig. 4 shows the noise attenuation achieved with IMM-AEKF seeker filter Average of 50 Monte Carlo simulation.

The robustness of IMM-AEKF seeker filter is evaluated by checking its performance in close loop with Monte Carlo simulation for (i) different interceptor-target engagement geometry, (ii) different target aspect ratio in the glint noise model, (iii) different mode transition probability matrix which is a design parameter for IMM.

	Δx	$\Delta \dot{x}$	Δy	$\Delta \dot{y}$	Δz	$\Delta \dot{z}$
Case No. 1	0.0800	0.2239	0.3375	5.9389	0.7259	10.7550
Case No. 4	0.0662	0.2022	0.1760	4.3645	0.3561	5.1017

Table 2 Percentage Fit Error

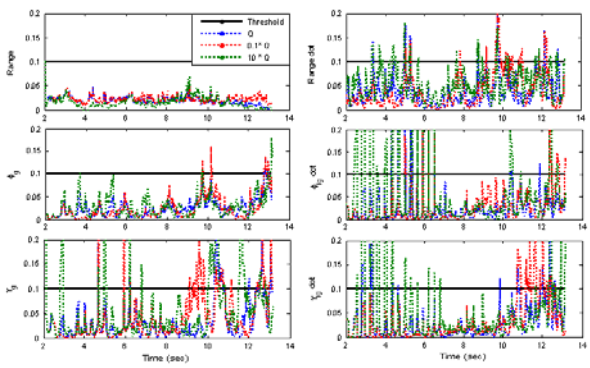

Figure 4 Noise attenuation by the filter with different process noise (Average of 50 Monte Carlo simulation)

Interceptor-target engagement geometry:

Fig.5 shows the histogram of miss distance achieved (IMM-AEKF) for 100 Monte-Carlo runs and for 12 cases. It can be seen from the distribution that the probability of achieving miss distance less than 10 meter is significantly high. Fig. 6 shows the state estimation errors for the relative positions along all the three axes along with the 1σ bounds in log scale averaged over 100 MC runs for all the 12 cases. It is clear that all the estimation errors are well within the bounds. Fig. 7 shows the evolution of the estimation errors for the range and range rate as more measurement samples are processed. The theoretical bound $(\frac{\sigma}{\sqrt{N}})$ shows that when there is no modeling error, the effect of noise decreases as more measurement samples are processed. It is clear from the figure that the effect of noise is reduced by both the filters. However, the noise attenuation at the end is not as significant as expected. Perhaps high sampling rates may solve the problem. The figures also show that the filter performance reaches a steady state after a while and further increase in measurement samples do not result in any performance improvement contrary to expectations that more measurements should improve filter performance. Similar observations are made for other measurements of RF seeker.

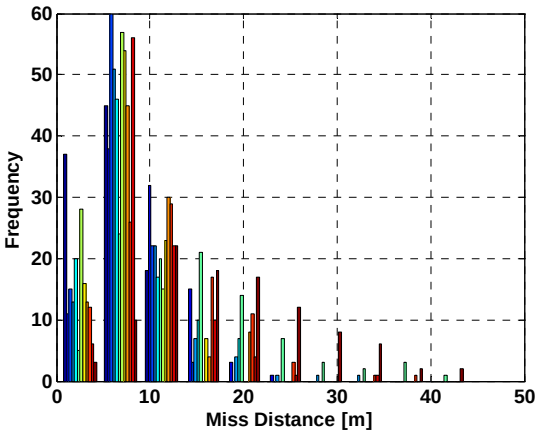

Figure 5 Histogram of Miss Distance (IMM-AEKF)

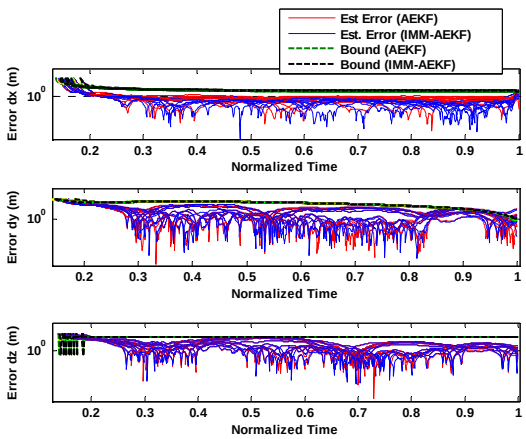

Figure 6 Comparison of theoretical bound with relative position estimation errors averaged over 100 Monte-Carlo runs – 12 cases

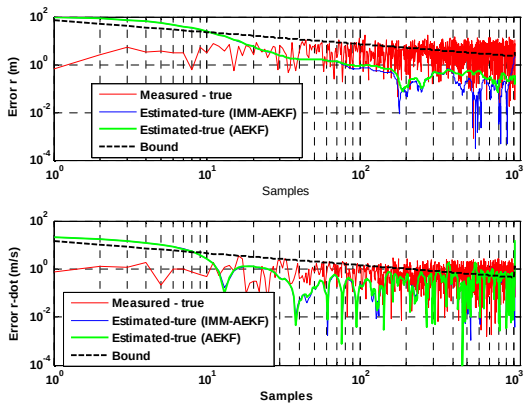

Figure 7 Comparison of theoretical bound with range and range rate estimation errors averaged over 100 Monte-Carlo runs – case 1

Target aspect ratio: Target aspect ratio (α_{target}) is a parameter which decides the intensity of glint noise in the measured seeker data. The study has been carried out by changing the α_{target} in 6 DOF simulation (FORTRAN code) and considering different values of α_{target} in the seeker filter model corresponding to each α_{target} value in 6 DOF code as shown in the Table 3 (keeping other parameters to their tuned values). These values of α_{target} are in the normally encountered range for ABTs. The results indicate that the close loop performance of seeker filter is best with α_{target} =0.2 as shown in the highlighted portion of Table 3.

α_{target} in 6dof sim code	α_{target} in seeker filter model	Flight Time (sec)	Miss Distance (m)	Closing Velocity (m/s)	Max Latax (g) pitch , yaw	Max Gimbal (deg) pitch , yaw	Impact Mach	Impact Ratio Vm/Vt
0.1	0.1	13.29	5.94	299	28 , 25	11 , 10	1.77	4.50
	0.2	13.29	5.41	299	28 , 25	10 , 10	1.77	4.50
	0.5	13.30	8.65	163	29 , 26	10 , 12	1.76	4.47
0.2	0.1	13.29	5.67	207	27 , 27	11 , 12	1.77	4.52
	0.2	13.29	5.59	405	28 , 27	11 , 5	1.77	4.50
	0.5	13.30	6.74	-135	29 , 26	10 , 12	1.75	4.47
0.5	0.1	13.29	18.40	133	28 , 27	11 , 12	1.78	4.54
	0.2	13.30	5.35	17	27 , 27	12 , 12	1.76	4.48
	0.5	13.30	12.99	-154	26 , 28	11 , 12	1.77	4.51

Table 3 Sensitivity w.r.t Target Aspect Ratio

Mode transition probability: Transition mode probability is a design parameter of IMM-AEKF. It permits transition from one model to another model. Initial mode probabilities are selected on the basis of target maneuver sojourn time. In the 2 model (CA and CJ) IMM seeker filter the mode transition probability matrix chosen is $p = \begin{bmatrix} 0.5 & 0.5 \\ 0.01 & 0.99 \end{bmatrix}$. This selection is based on observation that most of the time the target is in jerk mode and the probability of transition from acceleration mode to jerk mode is very high. However sensitivity of these elements on the performance of seeker filter and in turn the guidance performance has been studied and is shown in the Table 4 and in Fig. 8. The results indicate that the performance is better if $P_{11}<P_{22}$ (P_{11} is the probability of the target continuing with the first mode and P_{22} is the probability of the target continuing with the second mode).

q-q plot of the residual errors: This study is expected to reveal whether the residuals processed using the IMM-AEKF display Gaussian behavior or non-Gaussian behavior. MATLAB® based function 'qqplot' is used to generate quantile plots of the filter residuals for the following Markov transition probability matrix values:

i) $p = \begin{bmatrix} 0.5 & 0.5 \\ 0.01 & 0.99 \end{bmatrix}$ - assigning more probability to the CJ mode than CA mode

ii) $p = \begin{bmatrix} 0.99 & 0.01 \\ 0.5 & 0.5 \end{bmatrix}$ - assigning more probability to the CA mode than CJ mode

iii) $p = \begin{bmatrix} 0.5 & 0.5 \\ 0.5 & 0.5 \end{bmatrix}$ - assigning equal probabilities to the CA and CJ modes

Mode transition Probability Matrix 'P'	Flight Time (sec)	Miss Distance (m)	Closing Velocity (m/s)	Max Latax(g)	Max Gimb (deg)	Impact Mach	Impact Ratio Vm/Vt
P = [0.5 0.5; 0.01 0.99]	13.29	5.59	405	28 , 27	11 , 5	1.77	4.50
P1= [0.99 0.01; 0.01 0.99]	13.30	15.86	11	28 , 22	9 , 12	1.76	4.48
P2= [0.99 0.01; 0.5 0.5]	13.31	17.98	-124	29 , 24	9 , 13	1.75	4.45
P3= [0.5 0.5; 0.5 0.5]	13.29	6.31	405	29 , 26	10 , 12	1.76	4.48

Table 4 Sensitivity w.r.t Mode Transition Probability

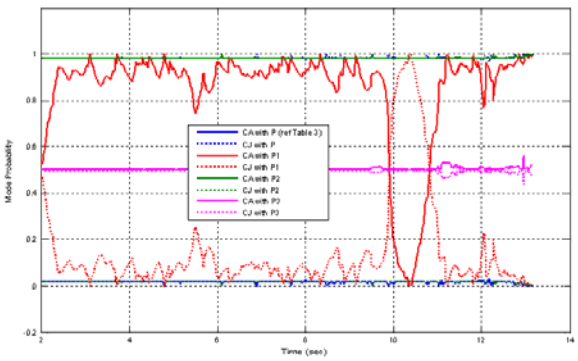

Figure 8 Estimated mode probabilities with different mode transition probabilities p (average of 50 monte carlo simulation)

Fig. 9 shows the q-q plot for above three cases using all the six measurement residuals of seeker filter. It is observed from the figure that the q-q plot of range residual display Gaussian behavior for (i). This means that residuals obtained has normal distribution only for this case. Similar observation made for range rate residual. In case of Gimbal angles and LOS rates, their respective qq plot indicates that these measurements are contaminated by non-Gaussian noise which is the actual case.

Estimation of algorithm cycle time in terms of flops: Estimation of floating point operations (flops) for one cycle is carried out for 2-model (CA and CJ) IMM-AEKF seeker filter. Since the latest version of MATLAB (version 6 onwards) does not support functions to estimate flops for given algorithms, a third party MATLAB toolbox named 'lightspeed' [11] is used for estimation of flops for seeker filter. Table 5 shows the approximate estimation of flops (computed manually) for each stage of IMM-AEKF algorithm and total flops per cycle.

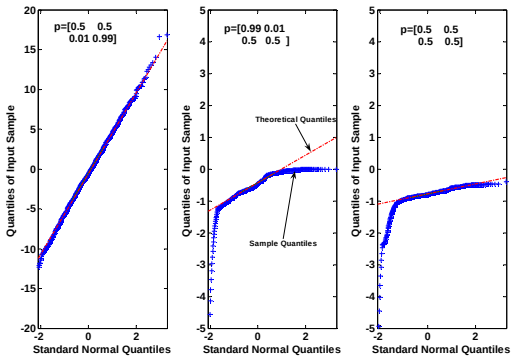

Figure 9 qq plot of range residual averaged over 100 Monte-Carlo runs for different markov transition probability (IMM-AEKF) - case 1

Stages of IMM-AEKF	Approximate flops
State interaction and mixing	2,286
Mode conditioned filtering	1,01,074
Likelihood computation	3228
Mode probability update	27
Overall State and Covariance Estimate	1092
Total flops per cycle	**1,07,707**

(The above computed flops exclude the filter initialization part)

Table 5 Approximate Computed flops of 2-model IMM-AEKF per cycle (MATLAB Version**)**

5 CONCLUDING REMARKS

In this paper, IMM based AEKF seeker filter is designed to operate in close loop homing guidance to track highly manoeuvring ABTs. The performance of the seeker filter is evaluated with six degree of freedom interceptor-target engagement simulation with seeker filter in closed guidance loop of the interceptor. Different filter performance criteria have been used to verify the performance of the seeker filter. The sensitivity/robustness of the seeker filter to various design parameters has been evaluated.

The seeker filter efficiently handles the various seeker noises and provides a smooth estimate of target states used to generate guidance command for missile. The miss distance achieved is within the acceptable limits.

ACKNOWLEDGEMENTS: This work was carried out as part of the sponsored project from DRDL Hyderabad. Authors would like to acknowledge the useful discussion and inputs from DRDL scientists of the TMS group during this work.

REFERENCES

[1] Lin C F, Modern Navigation, Guidance and Control Processing, Vol. 2, Prentice Hall, 1991.

[2] Paul Zarchan, Tactical and Strategic Missile Guidance: Third Edition, AIAA publishing, Virginia, 1997.

[3] Bar-Shalom Y and Chang K C, Tracking a Maneuvering Target using input estimation versus the Interacting Multiple Model Algorithm, IEEE Transactions on Aerospace and Electronics Systems, Vol. AES 26, No. 2, March, 1989.

[4] Wu W R, Target Tracking with Glint Noise, IEEE Transactions on Aerospace and Electronic Systems, Volume 29, No 1, pp 174-185, January, 1993.

[5] Kishore Mehrotra and Pravas R. Mahapatra, "A Jerk Model for Tracking Highly Maneuvering Targets", IEEE Trans. on Aero. and Elec. Sys., AES-33, pp 1094-1105, Oct. 1997.

[6] Bar-Shalom Y and Chang K C, Tracking a Maneuvering Target using input estimation versus the Interacting Multiple Model Algorithm, IEEE Transactions on Aerospace and Electronics Systems, Vol. AES 26, No. 2, March, 1989.

[7] S.K. Kashyap, V.P.S. Naidu, Jatinder Singh, Girija G. and Raol J.R., "Tracking of Multiple Targets using Interactive Multiple Model and Data Association Filter", Journal of Aerospace Sciences and Technologies, AeSI, Vol. 58, No. 2, pp 65-74, February, 2006.

[8] Ananthasayanam M R, Sarkar A K, Bhattacharya A, Tiwari P, Vorha P, Nonlinear Observer State Estimation From Seeker Measurements and Seeker-Radar Measurements Fusion, Paper No AIAA-2005-6066-CP, 2005.

[9] VPS Naidu, Shanthakumar N., Sudesh K. Kashyap, Girija G. and J.R. Raol, "Interacting Multiple Model Extended Kalman Filter for Tracking Target Executing Evasive Maneuvers", Paper No. 69, pp.285-290, International Radar Symposium India-2007 (IRSI-07), 10-13, Dec. 2007, Bangalore, India.

[10] VPS Naidu, Girija G. and J.R. Raol, "Estimation of Launch and Impact Point of a Flight Trajectory using U-D Kalman Filter/Smoother", Defence Science Journal, Vol. 5, No.4, pp.451-463, Oct. 2006

[11] Tom Minka, The Lightspeed Matlab toolbox, Efficient operations for Matlab programming,Version 2.2 , 17-Dec-2007, Microsoft Corporation.

[12] Kashyap S, Shanthakumar N and Girija G, IMM Based Augmented EKF for RF Seeker Filter, International Conference on Avionics Systems, February 2008, RCI, Hyderabad.

S.K. Kashyap received his Ph.D. degree in Electrical and Electronics Engineering from University of Mysore in 2008. He obtained M.E. in Electrical Engineering with specialization in Automatic Control and Robotics from M.S. University of Baroda, Gujarat. He is presently working at National Aerospace Laboratories, Bangalore as scientist E1. He is a recipient of NAL Young Scientist Award for Research in the year 2007. His areas of research are Multi Sensor Data Fusion for target tracking, Fuzzy logic based Decision fusion, Reconfiguration control, Neural network, Bayesian network and Situation assessment.

N Shantha Kumar obtained BE in Electrical Engineering from Bangalore university in 1985 and MTech in Aerospace engineering from IIT Mumbai in 1987. He is presently working at NAL, Bangalore as scientist F. For the last two decades he has worked in the area of system modeling and identification, target tracking and multi sensor data fusion.

VPS Naidu received his PhD in Electrical and Electronics Engineering from University of Mysore in 2009 and M.E. in Medical electronics from Anna University Chennai in 1997. He is working at National Aerospace Laboratories, Bangalore as scientist since December 2001 in the area of multi sensor data fusion for target tracking. His area of interest is in image fusion and tracking.

Girija G, received her Ph.D. from Bangalore University in 1996. She is presently working as Scientist G at National Aerospace Laboratories (NAL), Bangalore. Her areas of research are: modeling, parameter estimation of aerospace vehicles and multi sensor data fusion. She is a recipient of NAL Foundation Day Award for Research in the year 1995. She has published over 50 research papers. She is a member of Aeronautical Society of India